

Nonlinear internal gravity wave beams

By ALI TABAEI¹ AND T. R. AKYLAS²

¹Department of Civil and Environmental Engineering, Massachusetts Institute of Technology,
Cambridge, MA 02139, USA

²Department of Mechanical Engineering, Massachusetts Institute of Technology,
Cambridge, MA 02139, USA

(Received 30 August 2002 and in revised form 2 December 2002)

Based on linear inviscid theory, a two-dimensional source oscillating with frequency ω_0 in a uniformly stratified (constant Brunt–Väisälä frequency N_0) Boussinesq fluid induces a steady-state wave pattern, also known as St Andrew’s Cross, that features four straight wave beams stretching radially outwards from the source at angles $\pm \cos^{-1}(\omega_0/N_0)$ relative to the vertical. Similar wave beams are generated by oscillatory stratified flow over topography and also appear in simulations of thunderstorm-generated gravity waves in the atmosphere. Uniform plane-wave beams of infinite extent are in fact exact solutions of the nonlinear inviscid equations of motion, and this property is used here to study the propagation of finite-amplitude wave beams taking into account weak viscous and refraction effects. Oblique beams ($\omega_0 < N_0$) are considered first and an amplitude-evolution equation is derived assuming slow modulations along the beam direction. Remarkably, the leading-order nonlinear terms cancel out in this evolution equation and, as a result, the steady-state similarity solution of Thomas & Stevenson (1972) for linear viscous beams is also valid in the nonlinear régime. Moreover, for the same reason, nonlinear effects are found to be relatively unimportant for two-dimensional and axisymmetric beams that propagate nearly vertically ($\omega_0 \approx N_0$) in a Boussinesq fluid. Owing to the fact that the group velocity vanishes when $\omega_0 = N_0$, however, the transient evolution of nearly vertical beams takes place on a slower time scale than that of oblique beams; this is shown to account for the discrepancies between the steady-state similarity solution of Gordon & Stevenson (1972) and their experimental observations. Finally, the present asymptotic theory is used to study the refraction of nearly vertical nonlinear beams in the presence of background shear and variations in the Brunt–Väisälä frequency.

1. Introduction

Since gravity provides a preferred direction, the propagation of internal gravity waves in stratified fluids is anisotropic and gives rise to a variety of interesting and often intuitively unexpected phenomena. A classical example that clearly illustrates the effects of anisotropy, is the wave pattern induced by an oscillatory two-dimensional source in a uniformly stratified (constant Brunt–Väisälä frequency N_0) Boussinesq fluid; see, for example, Lighthill (1978, §4.4). In this instance, the dispersion relation of linear sinusoidal waves is such that the wave frequency ω is a function only of the angle θ that the wavenumber k makes with the vertical:

$$\omega = N_0 \sin \theta; \tag{1.1}$$

the group velocity $\mathbf{c}_g = \nabla_k \omega$, therefore, is perpendicular to the phase velocity $\mathbf{c} = (\omega/k^2)\mathbf{k}$, energy being transported along rather than perpendicularly to the wave crests. Hence, on kinematic grounds, we cannot expect cylindrical wavefronts from a two-dimensional oscillating source as would be the case in an isotropic medium where \mathbf{c} and \mathbf{c}_g are collinear. Instead, the induced steady-state internal wave pattern consists of four straight arms stretching radially outwards from the source along the characteristic directions $\pm \cos^{-1}(\omega_0/N_0)$ relative to the vertical, ω_0 being the source frequency. For each of these arms, the group velocity points outwards along the arm direction, as required by the radiation condition. This pattern, also known as ‘St Andrew’s Cross’, was verified experimentally in the laboratory by vibrating a horizontal cylinder in a stratified fluid tank (Mowbray & Rarity 1967).

The kinematic argument above furnishes the geometry of the wave pattern in the far field, but the precise structure of the wave beams emanating from the source as well as the near-field response depend on the details of the source and can be deduced only from a more complete solution. Assuming inviscid flow, Appleby & Crighton (1986), in particular, analysed the linear wave pattern induced by small rectilinear oscillations of a circular cylinder, including non-Boussinesq effects. Hurley (1997) discussed the analogous problem for an elliptical cylinder in a Boussinesq fluid and emphasized the need for including viscous effects to smooth out the singular behaviour of the inviscid solution along the characteristic lines tangent to the oscillating body.

A viscous steady-state similarity solution for obliquely propagating thin internal wave beams, generated by a line source oscillating with frequency $\omega_0 < N_0$, was presented by Thomas & Stevenson (1972) and was later extended by Makarov, Neklyudov & Chashechkin (1990) to more complex types of compact sources. Thomas & Stevenson (1972) also carried out laboratory experiments using a vibrating circular cylinder as forcing and found good agreement with their similarity solution which reveals that viscous beams broaden and their amplitude drops off as they propagate away from the source. In a more recent theoretical study extending the inviscid analysis of Hurley (1997) for a vibrating elliptic cylinder, Hurley & Keady (1997) obtained an approximate viscous solution which approaches the similarity solution of Thomas & Stevenson (1972) in the far field. The theoretical predictions of Hurley & Keady (1997) are in qualitative agreement with detailed experimental observations for a vertically oscillating elliptic cylinder reported by Sutherland & Linden (2002), although certain effects arising from the viscous boundary layer forming around the cylinder cannot be captured by the theory.

Internal wave beams akin to those seen in St Andrew’s Cross may also be generated by harmonic forcing other than small oscillations of a cylindrical object. Bell (1975), for instance, studied the steady-state wave pattern induced by a time-harmonic current of uniformly stratified Boussinesq fluid over a smooth bottom bump, for the purpose of modelling internal wave generation by tidal flows over sea-floor topography. In the reference frame moving with the current, the far-field response turns out to be a superposition of a finite number of V-shaped patterns, each being essentially half of a St Andrew’s Cross, with frequency equal to that of the background flow and all its higher harmonics below the Brunt–Väisälä frequency. These additional harmonics arise here because the oscillation amplitude of the bottom obstacle (in the reference frame moving with the background flow) need not be small compared to the width of the obstacle; in the small-amplitude limit, of course, the far-field response involves only one V-shaped pattern with frequency equal to that of the background flow, as was found by Appleby & Crighton (1986) and Hurley (1997).

In addition, there is now evidence from numerical simulations and field observations that a significant component of thunderstorm-generated gravity waves in the atmosphere is in the form of beam-like structures. Among several relevant numerical efforts, most notably Fovell, Durran & Holton (1992) and Alexander, Holton & Durran (1995) explored the generation of gravity waves by two-dimensional squall lines and put forward an interesting analogy with mechanical forcing. They suggested that oscillating updraft and downdraft cells within a squall line act as mechanical oscillators, similar to oscillating objects, and are responsible for the fan-like distribution of gravity wave beams seen in their simulations to propagate at various angles to the vertical. This ‘mechanical oscillator effect’ is further supported by three-dimensional simulations modelling actual storms (Lane, Reeder & Clark 2001; Piani *et al.* 2000). Of course, in three dimensions, mechanical oscillators act as point rather than line sources, and the generated gravity-wave disturbances turn out to be conical in shape, having nearly circular phase lines in planes of constant height, as indicated by the three-dimensional Green’s function derived by Voisin (1991). It is worth noting that such circular patterns have been identified in satellite images of the upper stratosphere and, based on the dispersion relation (1.1), Dewan *et al.* (1998) were able to link these gravity waves to isolated thunderstorms.

All existing theoretical models of St Andrew’s Cross and previous discussions of internal gravity wave beams in general are based on the linearized equations of motion. On the other hand, it so happens that uniform plane-wave beams of infinite extent that obey the linear dispersion relation (1.1) in a uniformly stratified Boussinesq fluid, are also solutions of the nonlinear inviscid equations of motion. This fact, which apparently had passed unnoticed before†, proves most useful here in setting up a finite-amplitude theory for the propagation of modulated wave beams that also takes into account weak viscous and refraction effects. While modulated wave beams are not exact nonlinear solutions, quite remarkably, it turns out that the leading-order nonlinear modulation terms cancel out in the amplitude equation governing the propagation of finite-amplitude beams. This implies that the steady-state similarity solution of Thomas & Stevenson (1972) for linear viscous beams is valid in the nonlinear regime as well.

The case of nearly vertically propagating beams with frequency close to the Brunt–Väisälä frequency, requires special treatment because, according to (1.1), the group velocity vanishes when $\theta = 0$; as a result, energy cannot be easily radiated away from the source and the transient response evolves on a relatively slow time scale. Assuming that the driving frequency is close to the Brunt–Väisälä frequency, an evolution equation for finite-amplitude slightly viscous beams is derived, taking into account non-Boussinesq effects as well as refraction effects owing to the presence of a weak background shear and small variations in the Brunt–Väisälä frequency. Again, the leading-order nonlinear modulation terms cancel out, the only nonlinearity coming from non-Boussinesq effects. Moreover, it is pointed out that these results carry over to nearly vertically propagating axisymmetric beams.

For the particular case of vertically propagating viscous beams generated by a line source oscillating at exactly the Brunt–Väisälä frequency in a Boussinesq fluid,

† It is, of course, well known (see, for example, Meid 1976) that linear sinusoidal wavetrains also satisfy the nonlinear equations of motion, and nonlinear corrections to such disturbances owing to non-Boussinesq effects were discussed by Kistovich, Neklyudov & Chashechkin (1990). We could not find, however, any reference to the fact that plane-wave beams, irrespective of their transverse profiles, are nonlinear solutions as well.

Gordon & Stevenson (1972) found a linear similarity solution which is also a possible steady state of the evolution equation derived here for finite-amplitude disturbances. The corresponding transient response, however, reveals that the approach to this steady state is rather slow owing to the fact that the group velocity of vertically propagating disturbances vanishes; this provides an explanation for the discrepancies noted by Gordon & Stevenson (1972) between their experimental observations and similarity solution.

Finally, based on the present asymptotic theory, we discuss refraction effects on nearly vertical nonlinear beams brought about by background shear and variations in the Brunt–Väisälä frequency.

2. Preliminaries

Consider internal gravity wave disturbances in an incompressible density-stratified fluid. We shall work with dimensionless variables throughout, using a characteristic length L associated with the waves as length scale, $1/N_0$ as time scale, N_0 being a typical value of the Brunt–Väisälä frequency, and a typical value $\bar{\rho}_0$ of the background density. The vertical (y -) coordinate is taken to point upwards and the background density $\bar{\rho}(y)$ is assumed to be stable ($\bar{\rho}_y < 0$). The Brunt–Väisälä frequency $N(y)$ then is given by

$$\bar{\rho}_y = -\beta \bar{\rho} N^2; \quad (2.1)$$

the Boussinesq parameter $\beta = LN_0^2/g$ is a measure of stratification, g being the acceleration due to gravity.

We find it convenient to work with the reduced density ρ and pressure p , defined so that $\beta \bar{\rho} \rho$ and $\bar{\rho} p$ are the density and pressure perturbations, respectively, from hydrostatic equilibrium. Taking into account (2.1), the governing equations for the velocity field \mathbf{u} , ρ and p then can be expressed as

$$\nabla \cdot \mathbf{u} = 0, \quad (2.2)$$

$$\rho_t + \mathbf{u} \cdot \nabla \rho - N^2(1 + \beta \rho)v = 0, \quad (2.3)$$

$$(1 + \beta \rho)(\mathbf{u}_t + \mathbf{u} \cdot \nabla \mathbf{u}) = -\nabla p - (\rho - \beta N^2 p)\mathbf{j} + \frac{\nu}{\bar{\rho}} \nabla^2 \mathbf{u} + \mathbf{F}, \quad (2.4)$$

where v denotes the vertical velocity component, \mathbf{j} is the unit vector along the vertical direction, ν stands for the inverse Reynolds number

$$\nu = \frac{\mu}{\bar{\rho}_0 L^2 N_0},$$

μ being the dynamic fluid viscosity, and \mathbf{F} represents externally applied forcing ($\bar{\rho} \mathbf{F}$ is force per unit volume).

In the Boussinesq approximation ($\beta \rightarrow 0$), we may write $\bar{\rho} = 1$ and if, furthermore, the background stratification is assumed uniform (constant Brunt–Väisälä frequency $N = 1$), the equation of mass conservation (2.3) and the momentum equation (2.4) simplify to

$$\rho_t + \mathbf{u} \cdot \nabla \rho - v = 0, \quad (2.5)$$

$$\mathbf{u}_t + \mathbf{u} \cdot \nabla \mathbf{u} = -\nabla p - \rho \mathbf{j} + \nu \nabla^2 \mathbf{u} + \mathbf{F}. \quad (2.6)$$

Consider now linear sinusoidal plane-wave disturbances in an inviscid uniformly stratified Boussinesq fluid. Taking the wavenumber $\mathbf{k} = k(\sin \theta, \cos \theta)$ to lie in the

(x, y)-plane at an angle θ to the vertical, it follows from (2.2) and the linearized forms of (2.5) and (2.6) (with $v = 0, \mathbf{F} = 0$) that

$$\mathbf{u} = i k (\cos \theta, -\sin \theta) \exp\{i(k\eta - \sin \theta t)\}, \quad (2.7)$$

$$(\rho, p) = (k, i \cos \theta) \exp\{i(k\eta - \sin \theta t)\}, \quad (2.8)$$

where

$$\eta = x \sin \theta + y \cos \theta, \quad (2.9)$$

and the wave frequency

$$\omega = \sin \theta \quad (2.10)$$

satisfies the dimensionless version of the dispersion relation (1.1).

Since, as already remarked, ω is independent of k , we may construct more general linear time-harmonic solutions with this same frequency, via superposition of (2.7) and (2.8), by fixing θ and varying k :

$$\mathbf{u} = Q_\eta (\cos \theta, -\sin \theta) e^{-i \sin \theta t} + \text{c.c.}, \quad (2.11)$$

$$(\rho, p) = (-i Q_\eta, i \cos \theta Q) e^{-i \sin \theta t} + \text{c.c.}, \quad (2.12)$$

where $Q(\eta)$ is a general complex amplitude and c.c. denotes complex conjugate.

It is important to note that the velocity field (2.11) is transverse to the η -direction; hence \mathbf{u} and ρ , being functions of η alone, do not vary along the direction of \mathbf{u} . As a result, the nonlinear convective-derivative terms in (2.5) and (2.6) vanish and, therefore, (2.11) and (2.12) are also nonlinear solutions to the inviscid equations of motion. While it is well known that sinusoidal plane-wave disturbances in a uniformly stratified Boussinesq fluid satisfy the nonlinear equations of motion, it is now clear that this property in fact holds for the more general class of disturbances (2.11) and (2.12).

In view of (2.9), the nonlinear solutions (2.11) and (2.12) describe uniform plane waves along

$$\xi = x \cos \theta - y \sin \theta, \quad (2.13)$$

but with a general profile along the η -direction. The frequency of oscillation (2.10) of these beam-like wave structures depends only on the angle θ that the η -direction makes with the vertical, precisely as the oscillation frequency of St Andrew's Cross. In the ensuing analysis, we shall make use of these nonlinear inviscid solutions to set up an asymptotic theory for the propagation of nonlinear wave beams that takes into account viscous and refraction effects in the presence of non-uniform background flow conditions.

3. Modulated nonlinear beams

According to experimental observations, internal wave beams due to an oscillating body are relatively thin, their width being comparable to the size of the source (see Lighthill 1978, §4.4), and numerical simulations reveal that the same is true for beam-like disturbances generated by thunderstorms (see, for example, Fovell *et al.* 1992). This suggests a boundary-layer-type approximation in which variations across the beam are assumed to be more rapid than those along the beam. This approach was taken by Thomas & Stevenson (1972) in deriving a steady-state viscous similarity solution for small-amplitude beams, and will also be adopted in the analysis below. Here, however, taking advantage of the nonlinear solutions (2.11) and (2.12)

for uniform inviscid beams noted earlier, we shall discuss slightly viscous beams of finite amplitude. Clearly, in the presence of variations along the beam direction, the nonlinear convective-acceleration terms in (2.5) and (2.6) no longer vanish, and it is of interest to ask how these nonlinearities would affect the beam evolution.

Focusing on a beam inclined at a finite angle θ to the horizontal, it is convenient to rotate the coordinate system and work in terms of η and ξ defined in (2.9) and (2.13), rather than x and y . Moreover, assuming that there are no variations in z , we introduce the streamfunction $\psi(\xi, \eta, t)$ so the incompressibility equation (2.2) is automatically satisfied. The mass- and momentum-conservation equations (2.5) and (2.6) (in a uniformly stratified Boussinesq fluid) then yield the following equations for ρ and ψ :

$$\rho_t + \sin \theta \psi_\eta + \cos \theta \psi_\xi + J(\rho, \psi) = 0, \quad (3.1)$$

$$\nabla^2 \psi_t - \sin \theta \rho_\eta - \cos \theta \rho_\xi + J(\nabla^2 \psi, \psi) - \nu \nabla^4 \psi = \chi_\eta - \zeta_\xi. \quad (3.2)$$

Here, χ and ζ are the components of the applied forcing \mathbf{F} along the ξ - and η -directions, respectively, and $J(a, b)$ stands for the Jacobian $a_\xi b_\eta - a_\eta b_\xi$.

In this formulation, the solution (2.11) and (2.12), corresponding to a uniform inviscid nonlinear beam away from the region of forcing ($\mathbf{F} = 0$), takes the form

$$\psi = Q(\eta) e^{i \sin \theta t} + \text{c.c.}, \quad (3.3)$$

$$\rho = i Q_\eta e^{i \sin \theta t} + \text{c.c.} \quad (3.4)$$

We now seek an asymptotic solution of (3.1) and (3.2) for a slightly viscous nonlinear wave beam with frequency $\omega = \sin \theta$ and amplitude that is slowly modulated along ξ and in time. For this purpose, we introduce the scaled variables

$$\xi \rightarrow \epsilon \xi, \quad \tau = \epsilon t, \quad (3.5)$$

$\epsilon \ll 1$ being a small parameter that controls the modulations. As will be seen, for viscous effects to be as important as modulation effects, ν must be $O(\epsilon)$, and we write

$$\nu = 2\alpha\epsilon, \quad \alpha = O(1). \quad (3.6)$$

We also expand ψ and ρ as follows

$$\psi = \{Q(\eta; \xi, \tau) e^{i\omega t} + \text{c.c.}\} + \epsilon \{Q_2(\eta; \xi, \tau) e^{2i\omega t} + \text{c.c.}\} + \epsilon Q_0(\eta; \xi, \tau) + \dots, \quad (3.7)$$

$$\rho = \{R(\eta; \xi, \tau) e^{i\omega t} + \text{c.c.}\} + \epsilon \{R_2(\eta; \xi, \tau) e^{2i\omega t} + \text{c.c.}\} + \epsilon R_0(\eta; \xi, \tau) + \dots, \quad (3.8)$$

anticipating that, in addition to the frequency $\omega = \sin \theta$ of the forcing

$$(\chi, \zeta) = (\hat{\chi}, \hat{\zeta}) e^{i\omega t} + \text{c.c.}, \quad (3.9)$$

the response also comprises higher harmonics and a mean term owing to nonlinear interactions precipitated by the modulations. Substituting expansions (3.7) and (3.8) in equations (3.1) and (3.2), collecting the various harmonics making use of the fact that $R = i Q_\eta + O(\epsilon)$ in view of (3.3) and (3.4), yields for the mean

$$Q_0 = -\frac{i}{\sin \theta} J(Q, Q^*), \quad (3.10a)$$

$$R_0 = \frac{1}{\sin \theta} \{J(Q_\eta, Q^*) + J(Q_\eta^*, Q)\}, \quad (3.10b)$$

where * denotes complex conjugate, and for the second harmonic

$$Q_{2\eta} = \frac{i}{\sin\theta} J(Q_\eta, Q), \quad (3.11a)$$

$$R_2 = i Q_{2\eta}. \quad (3.11b)$$

By equating first-harmonic terms and using (3.10) and (3.11), it then follows from (3.1), correct to $O(\epsilon^2)$:

$$\begin{aligned} R = & i Q_\eta + i \frac{\epsilon}{\sin\theta} (\cos\theta Q_\xi + i Q_{\eta\tau}) - i \frac{\epsilon^2}{\sin^2\theta} (Q_{\eta\tau} - i \cos\theta Q_\xi)_\tau \\ & + \frac{\epsilon^2}{\sin\theta} J(Q^*, Q_2)_\eta + i \frac{\epsilon^2}{\sin^2\theta} \{2J[J(Q_\eta, Q^*), Q] - (J[J(Q, Q^*), Q])_\eta\}. \end{aligned} \quad (3.12)$$

Similarly, equating first-harmonic terms in (3.2) gives to the same order of ϵ :

$$\begin{aligned} \sin\theta (i Q_\eta - R)_\eta + \epsilon (Q_{\eta\tau} - \cos\theta R_\xi - 2\alpha Q_{\eta\eta\eta}) + \epsilon^2 \{i \sin\theta Q_{\xi\xi} + J(Q_{2\eta\eta}, Q^*) \\ + J(Q_{\eta\eta}^*, Q_2) - J(Q_0, Q_{\eta\eta}) - J(Q, Q_{0\eta\eta})\} = \hat{\chi}_\eta - \epsilon \hat{\zeta}_\xi + O(\epsilon^3). \end{aligned} \quad (3.13)$$

Finally, inserting (3.12) into (3.13) and making further use of (3.10) and (3.11), we can eliminate R , Q_0 and Q_2 to obtain, after a considerable amount of algebra, a single evolution equation for $Q(\eta; \xi, \tau)$:

$$\begin{aligned} 2\epsilon(Q_{\eta\tau} - i \cos\theta Q_\xi - \alpha Q_{\eta\eta\eta})_\eta + i \epsilon^2 \sin\theta Q_{\xi\xi} + \frac{2i \epsilon^2}{\sin\theta} \{J[J(Q_\eta, Q), Q^*] \\ + J[J(Q^*, Q_\eta), Q] + J[J(Q, Q^*), Q_\eta]\}_\eta = \hat{\chi}_\eta - \epsilon \hat{\zeta}_\xi + O(\epsilon^3). \end{aligned} \quad (3.14)$$

Although not immediately obvious, it can be verified by expanding out the Jacobians that the nonlinear terms in (3.14) cancel out. This implies that linear dispersive and viscous effects dominate nonlinear modulation effects in spite of the fact that the response amplitude is $O(1)$. Interestingly, Dauxois & Young (1999) encountered the same combination of Jacobians as in (3.14) (a special case of the Jacobi identity) and reached a similar conclusion in their study of near-critical reflection of a finite-amplitude internal wave from a slope in a uniformly stratified Boussinesq fluid. It should be noted that the second-harmonic and mean terms in (3.10) and (3.11) are non-zero, however, and contribute $O(\epsilon)$ nonlinear corrections to the response.

As expected, the most effective means of driving a beam is by applying forcing in the beam direction, which is also the direction of \mathbf{u} and of energy transport. Moreover, since the forcing \mathbf{F} was assumed to be locally confined in x and y , $\hat{\chi}$ may be expressed in terms of the scaled far-field variable ξ as follows:

$$\hat{\chi}(\eta, \xi) \sim 2\epsilon f(\eta) \delta(\xi), \quad (3.15)$$

where $f(\eta)$ is locally confined in η .

Taking into account (3.15), it then follows from (3.14) that the amplitude of the primary harmonic, to leading order in ϵ , is governed by

$$Q_{\eta\tau} - i \cos\theta Q_\xi - \alpha Q_{\eta\eta\eta} = f(\eta) \delta(\xi). \quad (3.16)$$

This evolution equation reflects a balance between dispersive, viscous and forcing effects. The linear dispersive terms, in particular, are responsible for guiding the energy coming from the forcing in the direction of the beam: according to the first two terms in (3.16), disturbances $\propto \exp(i l \eta)$ propagate along ξ with the corresponding group velocity $\cos\theta/l$, consistent with the dispersion relation (2.10). The viscous term, on

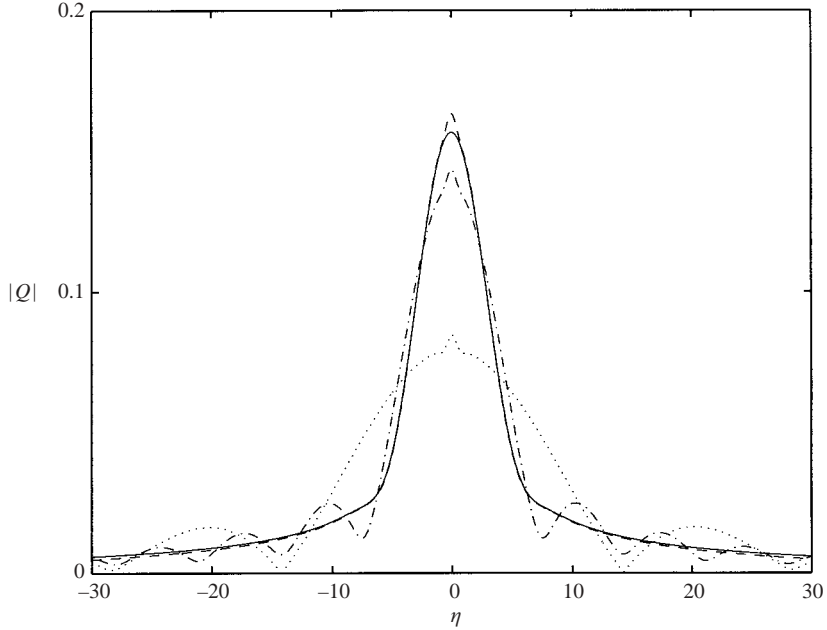


FIGURE 1. Cross-section of the response amplitude $|Q|$ at $\xi = 1$; —, steady-state response; \cdots , transient response at $\tau = 0.5$; $-\cdot-$, $\tau = 1$; $--$, $\tau = 2$.

the other hand, causes beams to broaden and decrease in amplitude away from the source.

A special steady-state solution of the evolution equation (3.16), corresponding to line forcing $f(\eta) = \delta(\eta)$, is the similarity solution of Thomas & Stevenson (1972):

$$Q = \frac{i}{2\pi \cos \theta} \left(\frac{\cos \theta}{\alpha} \right)^{1/3} \frac{1}{\xi^{1/3}} \int_0^\infty ds e^{-s^3} \exp \left\{ -is \left(\frac{\cos \theta}{\alpha} \right)^{1/3} \frac{\eta}{\xi^{1/3}} \right\}, \quad (3.17)$$

and can be readily obtained from the steady version of (3.16) using transforms. While the derivation of Thomas & Stevenson (1972) was based on linear theory, the fact that (3.16) remains valid in the nonlinear regime indicates that this similarity solution is actually not limited to small-amplitude disturbances. On the other hand, being a far-field solution, it is not valid in the vicinity of the forcing ($\xi \rightarrow 0$) and cannot be expected to capture phenomena arising from the details of the flow field close to the source, such as the viscous boundary layers forming around a vibrating cylinder (Sutherland & Linden 2002).

The steady-state response (3.17) at $\xi = 1$ for $\theta = \frac{1}{6}\pi$ and $\alpha = 1$ is plotted in figure 1 along with the corresponding transient response at various times τ . The transient response was obtained by solving (3.16) numerically, starting from rest and turning on the forcing impulsively at $\tau = 0$. (Details of the numerical procedure are given in the Appendix.) It is seen that $|Q|(\eta = 0, \xi = 1)$ is within 10% of the steady-state value after $\tau \approx 2$. Based on this time, we estimate that it would take about 1–2 min for a steady state to be established at distances from the source typical of those where measurements were made in the experiments of Thomas & Stevenson (1972) and Sutherland & Linden (2002).

4. Nearly vertical propagation

According to the dispersion relation (2.10), gravity wave beams propagate nearly vertically ($\theta \rightarrow \frac{1}{2}\pi$) when the driving frequency is close to the Brunt–Väisälä frequency ($\omega \rightarrow 1$). As is evident from (3.17), this is a singular limit, however, and requires special treatment. Physically, as $\theta \rightarrow \frac{1}{2}\pi$, it follows from (2.10) that the group velocity vanishes so energy cannot propagate easily away from the source, and the transient response evolves on a slower time scale than in the case of oblique propagation. The need for re-scaling as $\theta \rightarrow \frac{1}{2}\pi$ is also clear from (3.14) since the coefficient multiplying $Q_{\xi\eta}$ vanishes, suggesting that the $O(\epsilon^2)$ dispersive term involving $Q_{\xi\xi}$ should come into play in this limit. Here, we shall first derive the evolution equation governing two-dimensional nearly vertically propagating wave beams and then show that a similar equation applies in the analogous axisymmetric problem.

4.1. Two-dimensional disturbances

Employing the same boundary-layer approximation as before, we shall consider beams that vary slowly along the direction of propagation and, for this purpose, we introduce the stretched y -coordinate

$$Y = \epsilon y. \tag{4.1}$$

Also, in line with the remarks made earlier, the transient response here evolves more slowly than in the case of oblique propagation and the appropriate ‘slow’ time variable turns out to be

$$T = \epsilon^2 t, \tag{4.2}$$

rather than $\tau = \epsilon t$.

It is convenient to normalize the driving frequency to 1 and take the Brunt–Väisälä frequency to be

$$N^2 = 1 + \epsilon^2 q(Y), \tag{4.3}$$

thus allowing for the possibility of a small non-uniformity in the background stratification. Moreover, we may include weak non-Boussinesq effects by assuming that the Boussinesq parameter

$$\beta = \sigma\epsilon, \quad \sigma = O(1); \tag{4.4}$$

it then follows from (2.1) that the background density $\bar{\rho}$, to leading order, varies exponentially with height:

$$\bar{\rho} = e^{-\sigma Y}. \tag{4.5}$$

Finally, the choice

$$v = 2\alpha^2\epsilon^2, \quad \alpha = O(1), \tag{4.6}$$

ensures that viscous effects are as important as modulation and non-Boussinesq effects.

Returning to the governing equations (2.2)–(2.4), again we introduce the streamfunction ψ so as to satisfy (2.2) automatically. After eliminating p , implementing the scalings (4.1)–(4.6) in equations (2.3) and (2.4) then yields the following equation system, correct to $O(\epsilon^2)$, for $\psi(x, t; Y, T)$ and $\rho(x, t; Y, T)$:

$$\rho_t + \psi_x + \epsilon \{ J(\rho, \psi) + \sigma \rho \psi_x \} + \epsilon^2 (\rho_T + q \psi_x) = 0, \tag{4.7}$$

$$\begin{aligned} & \psi_{xxt} - \rho_x + \epsilon \{ J(\psi_{xx}, \psi) + \sigma (\rho \psi_{xt})_x \} \\ & + \epsilon^2 \left\{ \psi_{xxT} + \psi_{YYt} + \sigma (\rho J(\psi_x, \psi))_x - \sigma \psi_{Yt} - 2 \frac{\alpha^2}{\bar{\rho}} \psi_{xxxx} \right\} = F_y - G_x - \epsilon \sigma F, \end{aligned} \tag{4.8}$$

where F and G are, respectively, the horizontal and vertical components of the forcing \mathbf{F} and $J(a, b) = a_x b_Y - a_Y b_x$.

Next, ψ and ρ are expanded in a manner analogous to (3.7) and (3.8):

$$\psi = \{Q(x; Y, T) e^{it} + \text{c.c.}\} + \epsilon \{Q_2(x; Y, T) e^{2it} + \text{c.c.}\} + \epsilon Q_0(x; Y, T) + \dots, \quad (4.9)$$

$$\rho = \{R(x; Y, T) e^{it} + \text{c.c.}\} + \epsilon \{R_2(x; Y, T) e^{2it} + \text{c.c.}\} + \epsilon R_0(x; Y, T) + \dots. \quad (4.10)$$

Upon substituting these expansions in (4.7) and (4.8), collecting mean terms and using the fact that $R = i Q_x + O(\epsilon)$, we obtain

$$Q_{0x} + i J(Q, Q^*)_x = 0, \quad (4.11a)$$

$$R_{0x} - \{J(Q_x, Q^*) + J(Q_x^*, Q) + 2\sigma |Q_x|^2\}_x = 0. \quad (4.11b)$$

Apart from the mean-flow component induced by nonlinear interactions, we shall also allow for a possible $O(\epsilon^2)$ background shear flow $\epsilon^2 \bar{u}(Y)$:

$$\bar{u}(Y) = \bar{Q}_Y; \quad (4.12)$$

integrating (4.11) then

$$Q_0 = \bar{Q} - i J(Q, Q^*), \quad (4.13a)$$

$$R_0 = J(Q_x, Q^*) + J(Q_x^*, Q) + 2\sigma |Q_x|^2. \quad (4.13b)$$

Similarly, equating second-harmonic terms in (4.7) and (4.8) yields

$$Q_{2x} = i J(Q_x, Q) - \frac{1}{3} i \sigma Q_x^2, \quad (4.14a)$$

$$R_2 = -J(Q_x, Q) - \frac{1}{3} \sigma Q_x^2. \quad (4.14b)$$

Finally, collecting primary-harmonic terms in equations (4.7) and (4.8), we find

$$\begin{aligned} R &= i Q_x + i \epsilon^2 (R_T + q Q_x) + i \epsilon^2 \{J(R_0, Q) + J(R, Q_0) - J[J(Q_x, Q), Q^*] \\ &\quad - i J(Q_x^*, Q_2)\} + \frac{4}{3} i \epsilon^2 \sigma \{\sigma Q_x^2 Q_x^* + Q_x J(Q_x, Q^*)\}, \quad (4.15) \\ i Q_{xx} - R_x + \epsilon^2 \left(Q_{xxT} + i Q_{YY} - i \sigma Q_Y - 2 \frac{\alpha^2}{\rho} Q_{xxxx} \right) \\ &\quad + \epsilon^2 \{J(Q_{2xx}, Q^*) + J(Q_{xx}^*, Q_2) + J(Q_{0xx}, Q) + J(Q_{xx}, Q_0)\} \\ &\quad + i \epsilon^2 \sigma \{2 Q_x^* J(Q_x, Q) + 2 Q_x J(Q_x, Q^*) + 2 Q_x J(Q_x^*, Q) + \frac{5}{3} \sigma Q_x^2 Q_x^*\}_x \\ &= \hat{F}_y - \hat{G}_x - \epsilon \sigma \hat{F}, \quad (4.16) \end{aligned}$$

where

$$(F, G) = (\hat{F}, \hat{G}) e^{it} + \text{c.c.} \quad (4.17)$$

As before, making use of (4.13)–(4.15), it is possible to eliminate Q_0 , R_0 , Q_2 , R_2 and R from (4.16) and thus obtain a single evolution equation for Q . After considerable manipulation, it turns out (not unexpectedly this time) that all nonlinear modulation terms cancel out, the only remaining nonlinear terms in this equation coming from non-Boussinesq effects:

$$\begin{aligned} \{2i Q_{xT} + q Q_x + 2i \bar{u} Q_{xx} - \frac{1}{3} \sigma^2 Q_x^2 Q_x^*\}_x - Q_{YY} + \sigma Q_Y - i \frac{2\alpha^2}{\rho} Q_{xxxx} \\ = -i h_x \delta(Y) + i f[\delta'(Y) - \sigma \delta(Y)], \quad (4.18) \end{aligned}$$

where

$$(\hat{F}, \hat{G}) = \epsilon(f(x), \epsilon h(x)) \delta(Y) \quad (4.19)$$

is the far-field expression of the applied forcing. It is worth noting that small-amplitude forcing along the beam gives rise to an $O(1)$ response; this is a resonance phenomenon owing to the vanishing of the group velocity for vertically propagating beams.

The evolution equation (4.18) describes the generation of nearly vertical nonlinear wave beams by oscillatory forcing, including dispersive, viscous, non-Boussinesq as well as refraction effects under non-uniform background flow conditions. When all these effects come into play, we have to resort to numerical solution of (4.18), and specific examples will be discussed in §6. Here, in an effort to understand the various terms that enter in (4.18), we shall briefly consider certain limiting cases that are amenable to analytical treatment.

According to (4.18), ignoring viscous effects ($\alpha = 0$) and the background shear ($\bar{u} \equiv 0$), the steady-state response in a Boussinesq fluid ($\sigma = 0$) satisfies

$$q Q_{xx} - Q_{YY} = -i h_x \delta(Y) + i f \delta'(Y). \quad (4.20)$$

When $q > 0$ so the driving frequency is below the Brunt–Väisälä frequency according to (4.3), this is a forced wave equation in the (x, Y) -plane, and the response is a St Andrew's Cross with arms along the characteristic directions $dx/dY = \pm q^{1/2}$. On the other hand, if $q < 0$, (4.20) is elliptic and no propagation occurs above the Brunt–Väisälä frequency. This suggests that the nonlinear interaction term in (4.18), brought about by non-Boussinesq effects ($\sigma \neq 0$), as it amounts to replacing q by $q - \frac{1}{3}\sigma^2|Q_x|^2$, would possibly bend the arms of the St Andrew's Cross towards the vertical by an amount depending on the local response amplitude. We shall return to this point in §6.

In the special case of purely vertical line forcing ($f \equiv 0$, $h = \delta(x)$) at exactly the Brunt–Väisälä frequency ($q = 0$) in a Boussinesq fluid ($\sigma = 0$, $\bar{p} = 1$) with no background shear ($\bar{u} \equiv 0$), the response satisfies

$$2i Q_{xxT} - Q_{YY} - 2i\alpha^2 Q_{xxx} = -i\delta'(x)\delta(Y). \quad (4.21)$$

The corresponding steady-state solution takes the similarity form

$$Q_x = \frac{1}{4\pi} \frac{1-i}{\alpha} \frac{1}{\sqrt{Y}} \int_0^\infty ds \cos\left(s \frac{x}{\sqrt{Y}}\right) \exp((i-1)\alpha s^2) \quad (4.22)$$

and was first derived by Gordon & Stevenson (1972) based on linear theory; the present analysis, however, reveals that this solution is not limited to linear disturbances.

The transient solution of (4.21) and the approach to the steady state (4.22) will be further discussed in §5, in connection with the experimental observations of Gordon & Stevenson (1972).

4.2. Axisymmetric disturbances

We now turn attention to axisymmetric nearly vertical wave beams. As the analysis closely parallels that of §4.1, here we shall only sketch the main steps and, for simplicity, we shall assume Boussinesq flow ($\sigma = 0$, $\bar{p} = 1$) and purely vertical forcing ($\mathbf{F} = G \mathbf{j}$).

Under the same scalings, (4.1)–(4.3), as before, we shall again work with $\rho(r, t; Y, T)$ and the streamfunction $\psi(r, t; Y, T)$ defined so that

$$u = \frac{\epsilon}{r} \psi_Y, \quad v = -\frac{1}{r} \psi_r, \quad (4.23)$$

u being the velocity component along the direction of the radial coordinate r ; the incompressibility condition (2.2) is thus satisfied automatically.

It then follows from (2.3) and (2.4) that ρ and ψ satisfy, correct to $O(\epsilon^2)$:

$$\rho_t + \frac{1}{r} \psi_r + \frac{\epsilon}{r} J(\rho, \psi) + \epsilon^2 \left(\rho_T + \frac{q}{r} \psi_r \right) = 0, \quad (4.24)$$

$$\begin{aligned} & \left(\frac{\psi_r}{r} \right)_{rt} - \rho_r + \epsilon J \left(\frac{1}{r} \left(\frac{\psi_r}{r} \right)_r, \psi \right) \\ & + \epsilon^2 \left\{ \frac{1}{r} \psi_{YYt} + \left(\frac{\psi_r}{r} \right)_{rT} - 2\alpha^2 \left[\frac{1}{r} \left(r \left(\frac{\psi_r}{r} \right)_r \right)_r \right] \right\} = -G_r, \end{aligned} \quad (4.25)$$

assuming again that $v = 2\alpha^2\epsilon^2$ and $J(a, b) = a_r b_Y - a_Y b_r$ now being the Jacobian in the (r, Y) -plane.

After introducing expansions for ρ and ψ similar to those in (4.9) and (4.10), substituting these expansions into (4.24) and (4.25) yields for the mean and second-harmonic terms:

$$Q_0 = \frac{i}{r} J(Q^*, Q), \quad (4.26a)$$

$$R_0 = \frac{1}{r} (J(Q, V^*) + J(Q^*, V)), \quad (4.26b)$$

$$Q_{2r} = i J(Q, V), \quad (4.27a)$$

$$R_2 = \frac{1}{r} J(V, Q), \quad (4.27b)$$

where $V = -Q_r/r$ is the complex amplitude of the vertical velocity according to (4.23).

Similarly, collecting the primary-harmonic terms in equations (4.24) and (4.25), we have

$$R = -i V + i\epsilon^2 (R_T - qV) + i\epsilon^2 \left\{ \frac{1}{r} J(R_0, Q) + \frac{i}{r} \left(\frac{1}{r} J(Q_2, Q^*) \right)_r - \frac{i}{r} J(V, Q_0) \right\}, \quad (4.28)$$

$$\begin{aligned} & iV_r + R_r + \epsilon^2 \left\{ V_{rT} - \frac{i}{r} Q_{YY} - 2\alpha^2 \left(\frac{(rV_r)_r}{r} \right)_r \right\} - \epsilon^2 \left\{ J \left(\frac{1}{r} \left(\frac{Q_{2r}}{r} \right)_r, Q^* \right) \right. \\ & \left. - J \left(\frac{V_r^*}{r}, Q_2 \right) + J \left(\frac{1}{r} \left(\frac{Q_{0r}}{r} \right)_r, Q \right) - J \left(\frac{V_r}{r}, Q_0 \right) \right\} = \hat{G}_r. \end{aligned} \quad (4.29)$$

Following the same procedure as before, making use of (4.26)–(4.28), we can now eliminate Q_0 , R_0 , Q_2 , R_2 and R from (4.29) to obtain a single equation for Q . While this is a tedious task, the final result is relatively simple, for all nonlinear modulation terms cancel out once again. Specifically, we find that V satisfies the evolution equation

$$\frac{1}{r} \{ r(2i V_T + qV)_r \}_r - V_{YY} - 2i\alpha^2 \frac{1}{r} \left\{ r \left(\frac{(rV_r)_r}{r} \right)_r \right\} = \frac{i}{r} (rh_r)_r \delta(Y), \quad (4.30)$$

where

$$\hat{G} = \epsilon^2 h(r) \delta(Y) \tag{4.31}$$

denotes the applied forcing.

According to (4.30), in the special case of point forcing at exactly the Brunt–Väisälä frequency ($h(r) = \delta(r)$, $q = 0$), the steady-state response again takes a similarity form:

$$V = \frac{1}{8\pi} \frac{1-i}{\alpha} \frac{1}{Y} \int_0^\infty ds s J_0\left(s \frac{r}{\sqrt{Y}}\right) \exp((i-1)\alpha s^2), \tag{4.32}$$

J_0 being the Bessel function of order zero.

As would be expected, the axisymmetric response (4.32) drops off faster with vertical distance Y from the source (like $1/Y$) than its two-dimensional counterpart (4.22) which drops off like $1/\sqrt{Y}$.

5. Comparison with experiment

Gordon & Stevenson (1972) conducted laboratory experiments for the purpose of comparing against their steady-state similarity solution (4.22) of vertical wave beams. They used as a source a circular cylinder oscillating at the Brunt–Väisälä frequency in a stratified fluid tank, and measured the vertical displacement field across the disturbance at several heights above the source. The experimental observations were found to deviate significantly from the theoretical predictions, however, and Gordon & Stevenson (1972) attributed these discrepancies to reflections from the top and bottom walls of the tank. A revised theoretical solution, taking into consideration these reflections by using a system of image sources to satisfy inviscid boundary conditions at the walls, showed improved agreement with the experimental results.

Given that transients decay slowly for vertically propagating beams, we wish to revisit the experimental observations of Gordon & Stevenson (1972) in the light of the unsteady theory developed here. Figure 2 shows plots of the magnitude of the vertical velocity $|Q_x|$ across the beam at the normalized height $Y = 1$ for various values of the ‘slow’ time T , as obtained from solving the evolution equation (4.21) numerically with $\alpha = 1$ and the forcing turned on impulsively at $T = 0$ (see the Appendix for details), along with a plot of the corresponding steady-state solution (4.22) at this height. According to these plots, $|Q_x|(x = 0, Y = 1)$ is within 10% of the steady-state value after $T \approx 50$ or so.

Returning now to the non-dimensional variables adopted in §2, may select the characteristic length scale L so that the dimensional height of interest, y_0 say, above the source is normalized to $Y = 1$; this choice, combined with (4.5) taking $\alpha = 1$, then specifies

$$\epsilon = \left(\frac{\mu}{2\bar{\rho}_0 y_0^2 N_0} \right)^{1/4}. \tag{5.1}$$

Hence, based on the estimate obtained above ($T \approx 50$) for steady state to be reached at $Y = 1$, and recalling that $T = \epsilon^2 t$, the corresponding dimensional time t_0 after which steady state would be expected at y_0 turns out to be

$$t_0 \approx 50 \left(\frac{2\bar{\rho}_0}{\mu N_0} \right)^{1/2} y_0. \tag{5.2}$$

Specifically, Gordon & Stevenson (1972) worked with a stratified fluid having kinematic viscosity $\mu/\bar{\rho}_0 = 1.3 \text{ mm}^2 \text{ s}^{-1}$ and $N_0 = 1.12 \text{ s}^{-1}$, and made measurements

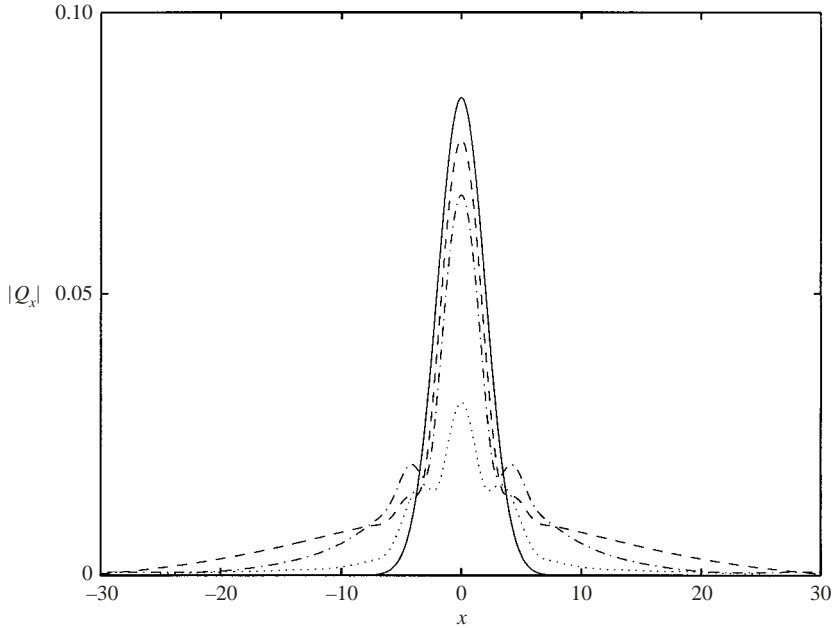


FIGURE 2. Cross-section of the vertical-velocity amplitude $|Q_x|$ at $Y = 1$; —, steady-state response; \cdots , transient response at $T = 1$; - - -, $T = 10$; - · -, $T = 50$.

of the response at several heights y_0 above the source in the range of 35–200 mm. At these stations, according to (5.1), it would be necessary to wait roughly between 30 min and 3 h after the source has been turned on for steady state to be established. On the other hand, as already remarked, in the experiments of Thomas & Stevenson (1972), who used a similar experimental set-up to generate oblique beams, steady state would be reached only within 1–2 min; moreover, Thomas & Stevenson (1972) report good agreement between experimental observations and the corresponding steady-state similarity solution (3.17).

This suggests that transient effects could have played a significant part in the experiments of Gordon & Stevenson (1972), and comparing their experimental data against unsteady responses predicted by the evolution equation (4.21), provides further evidence in support of this claim. Figure 3 makes a comparison between measurements of the magnitude of the vertical velocity across the beam at three heights above the cylinder and our theoretical predictions for the unsteady response at these stations at time $T = 1.2$, corresponding to 2 min after the source was turned on; the corresponding theoretical steady-state responses according to (4.22) are also shown on the same plot for reference. Since there is no direct way to link the vibrating cylinder used as a source in the experiments to the line forcing in (4.21), the theoretical response was multiplied by a constant factor so as to match the observed centreline response at the single station $y_0 = 35$ mm, but no other fitting of the theory to the experiment was made. At all three stations, the theoretical predictions are in very good agreement with the observations close to the centreline ($x = 0$) and capture reasonably well the secondary peaks of the measured responses away from the centreline. It is worth noting that these peaks decay rather slowly as is evident from figure 2; this would explain the discrepancies between the observations and the steady-state response which features no secondary peaks (see figure 3).

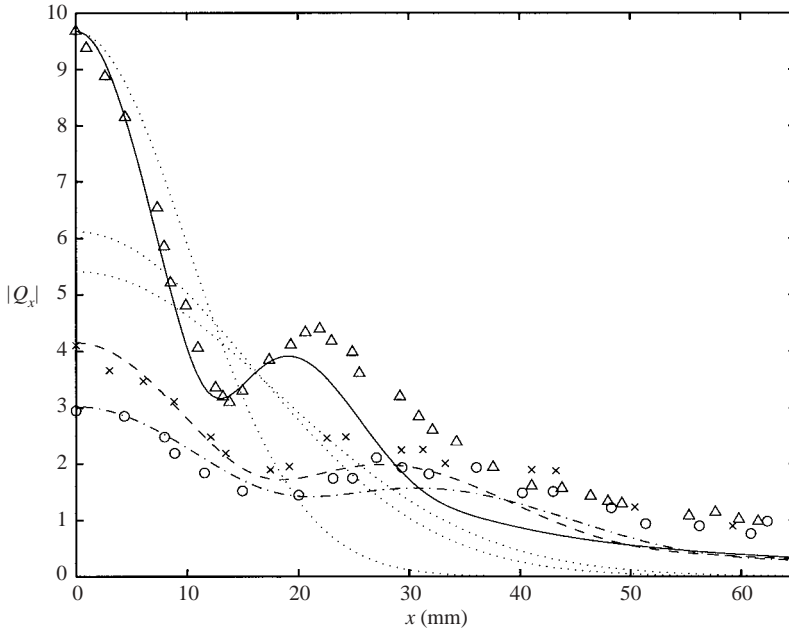


FIGURE 3. Comparison at three vertical distances (y_0) above the source between experimental observations of Gordon & Stevenson (1972) and theoretical unsteady response amplitude at $T=1.2$. Experimental results Δ , at $y_0 = 35$ mm; \times , 85 mm; \circ , 110 mm; transient response —, at $y_0=35$ mm; — —, 85 mm; - · - ·, 110 mm; ···, corresponding steady-state responses at these stations.

It was mentioned earlier that Gordon & Stevenson (1972), in an effort to explain their observations, worked out a revised steady-state theory, taking into account reflections from the top and bottom walls of their tank located 0.2 m from the source. Based on the present unsteady theory, however, according to (5.2), it would take several hours for the beams to reflect from the walls at steady state as assumed by Gordon & Stevenson (1972).

6. Refraction effects

The propagation of gravity wave beams in the atmosphere is influenced significantly by the presence of wind and variations in the Brunt-Väisälä frequency; the latter typically occur near the tropopause, the boundary between the troposphere and the stratosphere. As a result of non-uniform background flow conditions, the arms of St Andrew's Cross are no longer symmetrical owing to refraction effects, and numerical simulations of gravity wave beams generated by thunderstorms clearly show this asymmetric behaviour (Fovell *et al.* 1992; Lane *et al.* 2001).

We shall use the evolution equation (4.18) to discuss refraction effects on the propagation of finite-amplitude nearly vertical beams. This equation is solved numerically using a spectral technique as described in the Appendix. The only nonlinear term in (4.18) derives from non-Boussinesq effects, and it was suggested earlier that this term would possibly cause the direction of beam propagation to bend towards the vertical by an amount depending on the local wave amplitude. However, numerical solutions indicate that such a nonlinear effect, if present at all, is masked by the exponential variation of the disturbance with vertical distance Y brought about by

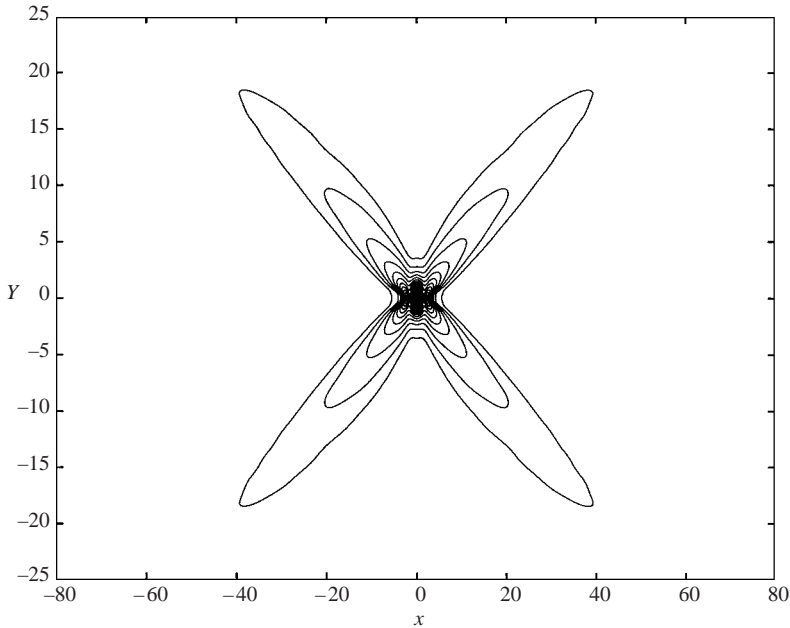


FIGURE 4. Contour plot of the amplitude of the vertical velocity $|Q_x|$ at $T = 4$ for a pattern generated by vertical line forcing at the origin under flow conditions corresponding to $\sigma = 0$, $q = 4$, $\alpha = 1$ and $\bar{u} = 0$.

the linear non-Boussinesq term in (4.18). As linear non-Boussinesq effects are familiar, in the interest of brevity, we shall focus here on Boussinesq flow ($\sigma = 0$, $\bar{\rho} = 1$) which also allows direct comparison with the simulations of Fovell *et al.* (1992).

We begin by showing in figure 4 a contour plot of the magnitude of the vertical velocity $|Q_x|$ at $T = 4$, as obtained from solving equation (4.18) numerically for a vertical line forcing at $x = Y = 0$ with $\alpha = 1$, $q = 4$ and $\bar{u} \equiv 0$; the driving frequency is thus below the Brunt–Väisälä frequency, assumed here to be uniform, and no background mean flow is present. Under such uniform flow conditions, no refraction takes place; all four beams propagate symmetrically along the directions $dx/dY = \pm 2$ as in a St Andrew's Cross, although the broadening of the beams away from the source caused by viscous effects is quite evident here.

It is interesting to contrast figure 4 with figure 5 which shows a similar contour plot for the pattern generated under the same flow conditions as above, but in the presence of variable Brunt–Väisälä frequency, $q = 4 - \frac{3}{4}Y$. Here, the fact that the Brunt–Väisälä frequency decreases with height inhibits the propagation of the two beams above the source, and the level $Y = \frac{16}{3}$ where the driving frequency matches the local Brunt–Väisälä frequency ($q = 0$) forms a barrier at which the beams are reflected since no propagation is possible beyond this barrier ($q < 0$). On the other hand, the two beams below the source bend away from the vertical owing to refraction, as they propagate into a region of increasing Brunt–Väisälä frequency.

Turning next to the effects of a background flow, figure 6 shows a contour plot of the disturbance generated under the same flow conditions as in figure 4, but in the presence of a uniform mean flow $\bar{u} = 2$. The main effect of the background flow is to tilt all four beams towards the flow direction so the two beams to the right (left)

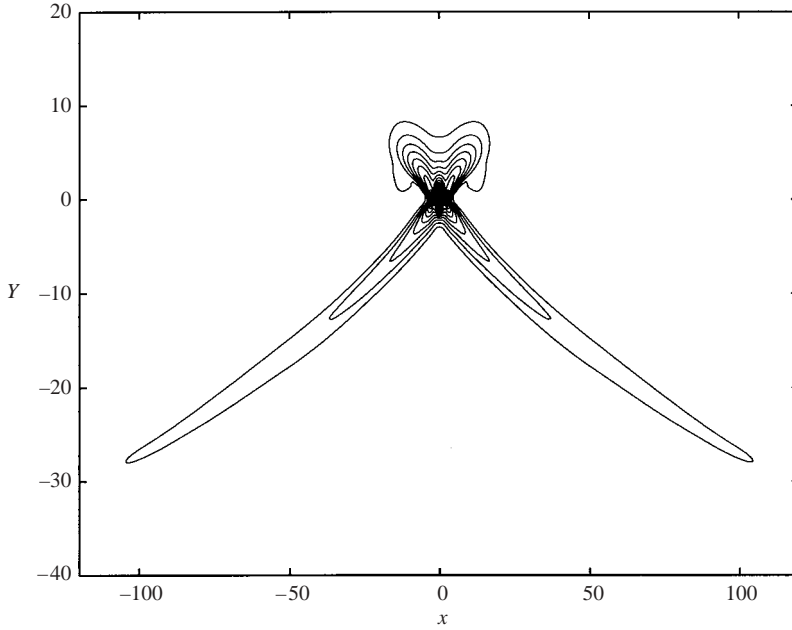


FIGURE 5. Contour plot of the amplitude of the vertical velocity $|Q_x|$ at $T = 4$ for a pattern generated by vertical line forcing at the origin under flow conditions corresponding to $\sigma = 0$, $q = 4 - \frac{3}{4}Y$, $\alpha = 1$ and $\bar{u} = 0$.

of the source are brought closer to the horizontal (vertical); moreover, the mean flow enhances (inhibits) propagation of the beams to the right (left) of the source.

These effects were also seen in the simulations of Fovell *et al.* (1992) and result from the Doppler shifting of the dispersion relation (2.10) by the mean flow:

$$\omega = \sin \theta + \bar{u} k_x, \tag{6.1}$$

k_x being the streamwise wavenumber component. Since $k_x > 0$ ($k_x < 0$) for the two beams to the right (left) of the source, $\sin \theta$ decreases (increases) in the presence of the mean flow so as to satisfy (6.1); hence, the beams to the right (left) of the source tilt away (towards) the vertical. Also, since the group velocity increases as the beam direction moves away from the vertical, it is natural for the right-hand beams to have propagated farther than the left-hand beams in figure 6.

The above reasoning may also be used to interpret the effects of a background shear flow. Figure 7, in particular, shows a contour plot of the disturbance generated under the same flow conditions as in figure 6, but with some shear added to the uniform mean flow:

$$\bar{u} = 2 + 0.1Y. \tag{6.2}$$

The pattern is now entirely asymmetrical. Since the background flow increases with height, the upper right-hand beam is tilted further away from the vertical as it encounters an increasing background flow, and has propagated farther than the lower right-hand beam. Similarly, the upper left-hand beam is pushed more towards the vertical and has propagated less than the lower left-hand beam which encounters an increasing background flow.

The forcing in all the computations reported above was taken to be vertical so any asymmetry of the generated patterns derives solely from the background flow

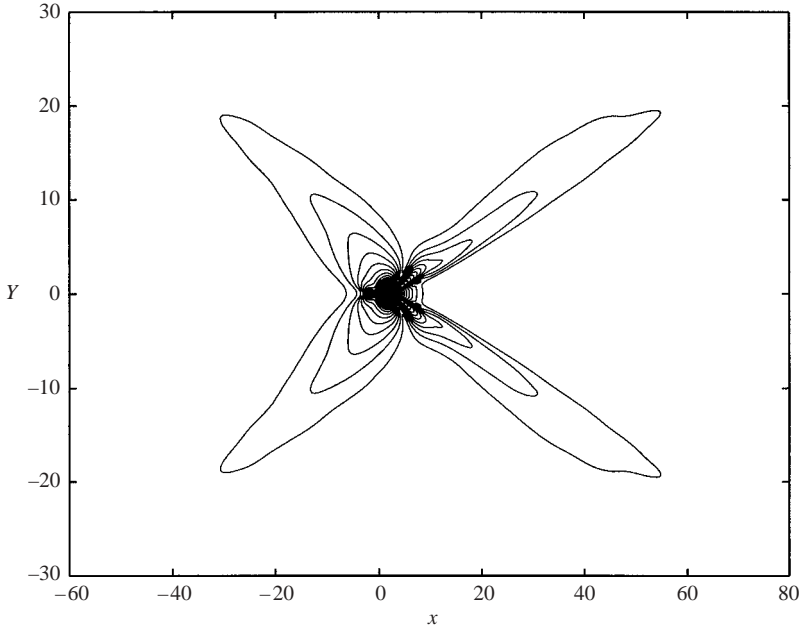


FIGURE 6. Contour plot of the amplitude of the vertical velocity $|Q_x|$ at $T = 4$ for a pattern generated by vertical line forcing at the origin under flow conditions corresponding to $\sigma = 0$, $q = 4$, $\alpha = 1$ and $\bar{u} = 2$.

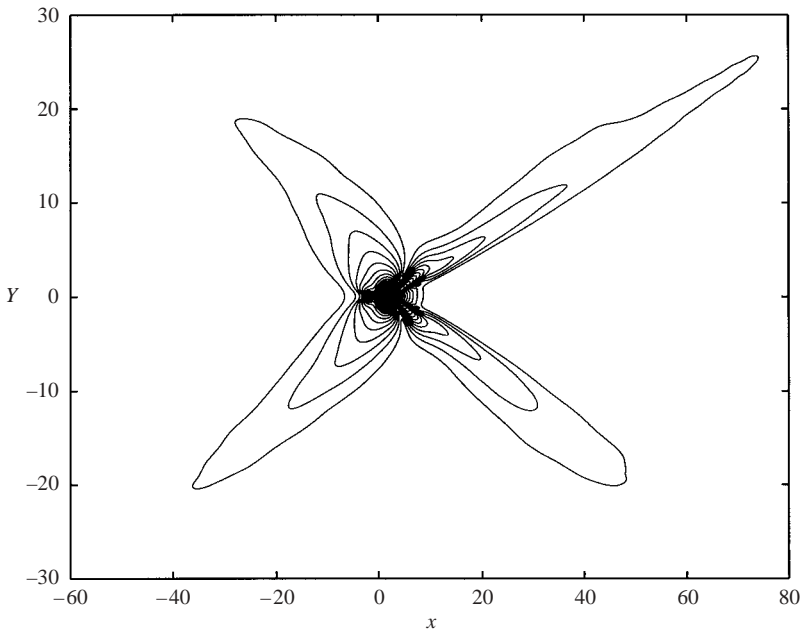


FIGURE 7. Contour plot of the amplitude of the vertical velocity $|Q_x|$ at $T = 4$ for a pattern generated by vertical line forcing at the origin under flow conditions corresponding to $\sigma = 0$, $q = 4$, $\alpha = 1$ and $\bar{u} = 2 + 0.1Y$.

conditions. We also briefly explored oblique forcing as another source of asymmetry. It turns out that the beams which are predominantly excited are those closer to the direction of the forcing, consistent with the findings of Fovell *et al.* (1992).

7. Final remarks

We have proposed an asymptotic theory for the propagation of finite-amplitude gravity wave beams in nearly uniformly stratified flow. Quite remarkably, nonlinear effects turn out to be relatively unimportant for both two-dimensional and axisymmetric wave beams, which explains the success of previous studies interpreting results from fully numerical simulations and field observations on the basis of linear theory.

There are, nevertheless, at least two instances in which nonlinearity is expected to play an important part. Specifically, in the case of two-dimensional nearly hydrostatic wave beams that propagate almost horizontally ($\sin \theta = \epsilon \ll 1$), the scaled horizontal coordinate $X = \epsilon x$ and the ‘slow’ time $\tau = \epsilon t$ are appropriate. It then follows from (2.5) and (2.6) that the streamfunction $\psi(y; X, \tau)$ and reduced density $\rho(y; X, \tau)$ satisfy (for a Boussinesq fluid with $\nu = 2\alpha\epsilon$) to leading order

$$\rho_\tau + \psi_y + \psi_X + J(\rho, \psi) = 0, \tag{7.1}$$

$$\psi_{yy\tau} - \rho_y - \rho_X - 2\alpha\psi_{yyy} + J(\psi_{yy}, \psi) = F_y - G_X, \tag{7.2}$$

where ϵF and G denote, respectively, the horizontal and vertical components of the forcing, and $J(a, b) = a_X b_y - a_y b_X$ now stands for the Jacobian in the (X, y) -plane. It is important to note that, unlike (4.7) and (4.8), the equation system (7.1) and (7.2) remains fully nonlinear after rescaling so here nonlinearity is expected to have an $O(1)$ effect.

The second instance in which nonlinearity turns out to be important owing to a stronger interaction of the primary harmonic with the induced mean flow, is that of nearly vertically propagating non-axisymmetric beams; this case would arise, for example, when a point source oscillates with frequency close to the Brunt–Väisälä frequency in the presence of a horizontal background flow.

Both of these flow configurations are under current investigation and details will be reported elsewhere.

The authors wish to thank Professors R. H. J. Grimshaw and V. I. Shrira for a number of very helpful suggestions. Also several useful discussions on this and related topics with Dr Robert Beland and his group at the Air Force Research Laboratory in Hanscom AFB are gratefully acknowledged. Finally, we are grateful to an anonymous referee who reviewed the manuscript very thoroughly and made several suggestions that improved the final version of this paper.

This work was supported by the Air Force Office of Scientific Research, Air Force Materials Command, USAF, under Grant F49620-01-1-001 and by the National Science Foundation Grant DMS-0072145.

Appendix. Numerical procedures

Here we give details of the numerical procedures used to solve the evolution equations (3.16) and (4.18).

The steady-state similarity solutions (3.17) and (4.22) were computed by simply evaluating the integrals involved via the trapezoidal rule. Transient responses were

obtained by spectral techniques using a fast Fourier transform. For this purpose, the computational domain was set between 0 and 2π by suitable rescaling. In all cases, forcing was turned on impulsively, taking the response to be zero initially.

Since (3.16) is a linear equation with constant coefficients, it was solved by working in the Fourier domain where the Fourier transform $\mathcal{F}(Q)$ can be readily obtained analytically as a function of time, and finally inverting $\mathcal{F}(Q)$ numerically. Care was taken to ensure that the spatial domain used was large enough not to allow reflections from the boundaries, and the spatial resolution was varied accordingly (from 512×512 to 2048×2048 Fourier modes) so that the transform of the disturbance did not reach the boundaries of the Fourier domain. Specifically, for the results shown in figure 1, 2048×2048 Fourier modes were used in the spatial domain $-30 < \xi < 30$, $-60 < \eta < 60$.

For the purpose of solving the evolution equation (4.18) numerically, it proved more convenient to work with the vertical velocity amplitude $V = -Q_x$ and use the following transformation

$$V = \exp\left(\frac{1}{2}\sigma Y\right) \tilde{V}, \quad (\text{A } 1)$$

to remove the term involving V_Y . Implementing (A 1) after differentiating (4.18) once with respect to x , the transformed variable \tilde{V} satisfies the following equation

$$\begin{aligned} \{2i\tilde{V}_T + q\tilde{V} + 2i\bar{u}\tilde{V}_x - \frac{1}{3}\sigma^2 \exp(\sigma Y)\tilde{V}^2\tilde{V}^*\}_{xx} - \tilde{V}_{YY} + \frac{1}{4}\sigma^2\tilde{V} - 2i\alpha^2 \exp(\sigma Y)\tilde{V}_{xxxx} \\ = i \exp\left(-\frac{1}{2}\sigma Y\right)\{h_{xx}\delta(Y) + f_x[\sigma\delta(Y) - \delta'(Y)]\}. \end{aligned} \quad (\text{A } 2)$$

To advance \tilde{V} in time, we apply the split-step pseudospectral method of Lo & Mei (1985, 1987) to (A 2). Specifically, at each time step, the nonlinear terms as well as the linear terms with variable coefficients are approximated by centred finite differences while the rest of the linear terms are treated by Fourier transform. For the computations presented in §6, in particular, a computational grid with 512×512 points and the time step $\Delta T = 0.001$ were used. The same computations were also repeated using $\Delta T = 0.01$ on a 256×256 grid with no significant change in the results.

Since the response vanishes far from the source and the forcing is locally confined, it follows from (A 2), by integrating with respect to the cross-beam direction, that \tilde{V} satisfies a constraint of the form

$$\left(\frac{\partial^2}{\partial Y^2} - \frac{\sigma^2}{4}\right) \int_{-\infty}^{\infty} \tilde{V} \, dx = 0, \quad (\text{A } 3)$$

which combined with the fact that $\tilde{V} \rightarrow 0$ as $Y \rightarrow \pm\infty$ implies that

$$\int_{-\infty}^{\infty} \tilde{V} \, dx = 0, \quad (\text{A } 4)$$

and hence the value of $\mathcal{F}(\tilde{V})$ at zero wavenumber in the cross-beam direction must vanish. Using a Fourier transform to integrate (A 2) allows us to satisfy this constraint exactly.

REFERENCES

- ALEXANDER, M. J., HOLTON, J. R. & DURRAN, D. R. 1995 The gravity wave response above deep convection in a squall line simulation, *J. Atmos. Sci.* **52**, 2212–2226.
 APPLEBY, J. C. & CRIGHTON, D. G. 1986 Non-Boussinesq effects in the diffraction of internal waves from an oscillating cylinder. *Q. J. Mech. Appl. Maths* **39**, 209–231.

- BELL, T. H. 1975 Lee waves in stratified flows with simple harmonic time dependence *J. Fluid Mech.* **67**, 705–722.
- DAUXOIS, T. & YOUNG, W. R. 1999 Near-critical reflection of internal waves. *J. Fluid Mech.* **390**, 271–295.
- DEWAN, E. M., PICARD, R. H., O'NEIL, R. R., GARDINER, H. A. & GIBSON, J. 1998 MSX satellite observations of thunderstorm-generated gravity waves in mid-wave infrared images of the upper stratosphere. *Geophys. Res. Lett.* **25**, 939–942.
- FOVELL, R., DURRAN, D. & HOLTON, J. R. 1992 Numerical simulations of convectively generated stratospheric gravity waves. *J. Atmos. Sci.* **49**, 1427–1442.
- GORDON, D. & STEVENSON, T. N. 1972 Viscous effects in a vertically propagating internal wave. *J. Fluid Mech.* **56**, 629–639.
- HURLEY, D. G. 1997 The generation of internal waves by vibrating elliptic cylinders. Part 1. Inviscid solution. *J. Fluid Mech.* **351**, 105–118.
- HURLEY, D. G. & KEADY, G., 1997 The generation of internal waves by vibrating elliptic cylinders. Part 2. Approximate viscous solution. *J. Fluid Mech.* **351**, 119–138.
- KISTOVICH, A. V., NEKLYUDOV, V. I. & CHASHECHKIN, Y. D. 1990 Nonlinear two-dimensional internal waves generated by a periodically moving source in an exponentially stratified medium. *Izv. Atmos. Ocean. Phys.* **26**, 771–776.
- LANE, T. P., REEDER, M. J. & CLARK, T. L. 2001 Numerical modeling of gravity wave generation by deep tropical convection. *J. Atmos. Sci.* **58**, 1249–1274.
- LIGHTHILL, M. J., 1978 *Waves in Fluids*. Cambridge University Press.
- LO, E. & MEI, C. C., 1985 A numerical study of water-wave modulation based on a higher-order nonlinear Schrödinger equation. *J. Fluid Mech.* **150**, 395–416.
- LO, E. & MEI, C. C. 1987 Slow evolution of nonlinear deep water waves in two horizontal directions: a numerical study. *Wave Motion* **9**, 245–259.
- MAKAROV, S. A., NEKLYUDOV, V. I. & CHASHECHKIN, Y. D. 1990 Spatial structure of two-dimensional and monochromatic internal-wave beams in an exponentially stratified liquid. *Izv. Atmos. Ocean. Phys.* **26**, 548–554.
- MIED, R. R. 1976 The occurrence of parametric instabilities in finite-amplitude internal gravity waves. *J. Fluid Mech.* **78**, 763–784.
- MOWBRAY, D. E. & RARITY, B. S. H., 1967 A theoretical and experimental investigation of the phase configuration of internal waves of small amplitude in a density stratified liquid. *J. Fluid Mech.* **28**, 1–16.
- PIANI, C., DURRAN, D., ALEXANDER, M. J. & HOLTON, J. R. 2000 A numerical study of three-dimensional gravity waves triggered by deep tropical convection and their role in the dynamics of the QBO. *J. Atmos. Sci.* **57**, 3689–3702.
- SUTHERLAND, B. R. & LINDEN, P. F. 2002 Internal wave excitation by a vertically oscillating elliptical cylinder. *Phys. Fluids* **14**, 721–731.
- THOMAS, N. H. & STEVENSON, T. N. 1972 A similarity solution for viscous internal waves. *J. Fluid Mech.* **54**, 495–506.
- VOISIN, B. 1991 Internal wave generation in uniformly stratified fluids. Part 1. Green's function and point sources. *J. Fluid Mech.* **231**, 439–480.